IEEE Photonics Journal
An IEEE Photonics Society Publication

Open Access

Grating Coupler for an On-Chip Lithium Niobate Ridge Waveguide

Volume 9, Number 1, February 2017

Muhammad Shemyal Nisar
Xiangjie Zhao
An Pan
Shui Yuan
JinSong Xia

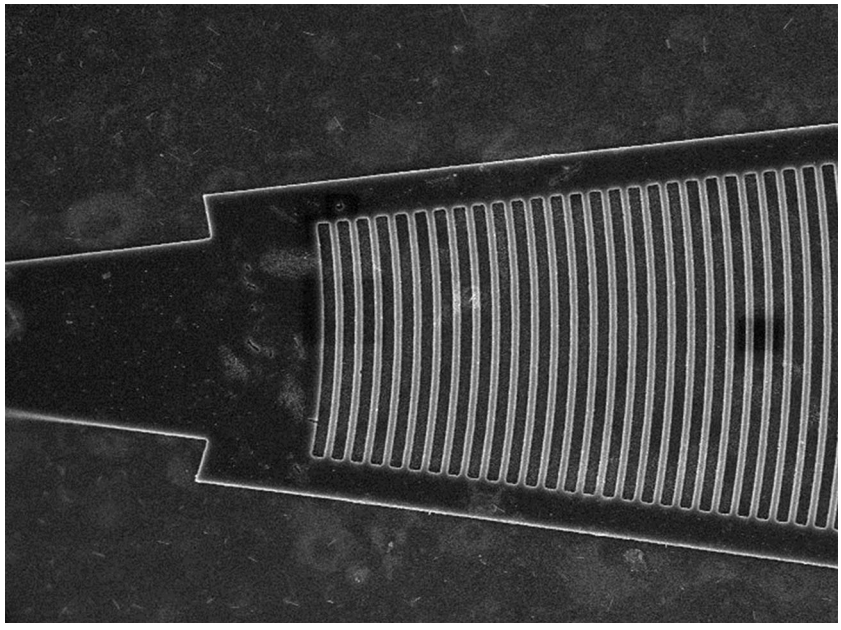

DOI: 10.1109/JPHOT.2016.2630314
1943-0655 © 2016 IEEE

IEEE photonics SOCIETY

IEEE

Grating Coupler for an On-Chip Lithium Niobate Ridge Waveguide

Muhammad Shemyal Nisar, Xiangjie Zhao, An Pan, Shui Yuan, and JinSong Xia

Wuhan National Laboratory of Optoelectronics, School of Electronic Information and Communications Huazhong University of Science and Technology, Wuhan 430074, China

DOI:10.1109/JPHOT.2016.2630314
1943-0655 © 2016 IEEE. IEEE. Translations and content mining are permitted for academic research only. Personal use is also permitted, but republication/redistribution requires IEEE permission. See http://www.ieee.org/publications_standards/publications/rights/index.html for more information.

Manuscript received September 30, 2016; revised November 10, 2016; accepted November 14, 2016. Date of publication December 1, 2016; date of current version February 13, 2017. This work was supported in part by the 863 Project under Grant 2015AA016904, in part by the National Natural Science Foundation of China under Grant 61335002 and Grant 11574102, in part by the Major State Basic Research Development Program of China under Grant 2013CB632104 and Grant 2013CB933303, and in part by the Specialized Research Fund for the Doctoral Program of Higher Education under Grant 20110142120059. *(M. S. Nisar and X. Zhao contributed equally to this work.)* Corresponding author: J. Xia (jinsongxia@gmail.com).

Abstract: We report simulation and fabrication of a grating coupler for coupling of light between an on-chip lithium niobate ridge waveguide and an optical fiber. A grating coupler with an insertion loss of less than 10 dB for C-band frequencies (1530–1565 nm) was achieved.

Index Terms: Lithium niobate thin film, microfabrication, grating coupler.

1. Introduction

Lithium Niobate is an important opto-electronic material with a variety of uses including higher frequency generation [1]–[4], interferometers [5]–[8], modulators [9]–[12], optical amplifier [13]–[15], switches [16], [17], etc. Lithium Niobate is a special ferroelectric material whose characteristics due to its unique crystal structure include Pyroelectric Effect, Piezoelectric and Converse Piezoelectric Effect, Birefringent Permittivity, Pockels Effect, Elasticity, Photo- elastic Effect, Bulk Photovoltaic Effect, and Photorefractive Effect [18].

Lithium Niobate is one of the hardest materials to etch, which means that etching process imposes considerable constraints on the design parameters and especially on the process adopted for fabrication [19], [20], [21]. Moreover, fabricating an on-chip device adds further limitations on the process as care must be taken to save the layer of Silicon Dioxide from being etched. This rules out most of the wet etching techniques available in the literature [19], [20], [21], which is usually employed for bulk material.

Vertical or near vertical coupling is a well-established method for coupling between optical fibre and submicron structures [23], with techniques ranging from simple 1-D photonic crystals to full pledge 3-D photonic crystals [24], [25] used to vertically couple light between optical fibre and nano-structures. The technique has also been employed for bulk Lithium Niobate systems as well [26]. On the other hand, there is no known report on such a structure for an on-chip Lithium Niobate with Silicon Dioxide substrate and Lithium Niobate handle wafer. The grating coupler would be useful for those situations where fiber-end coupling is not possible or feasible.

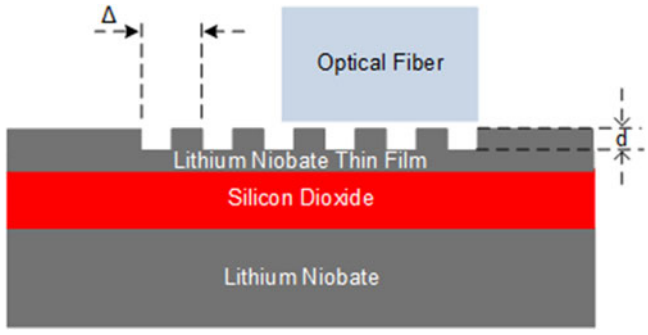

Fig. 1. Simulation layout and design parameters of Lithium Niobate.

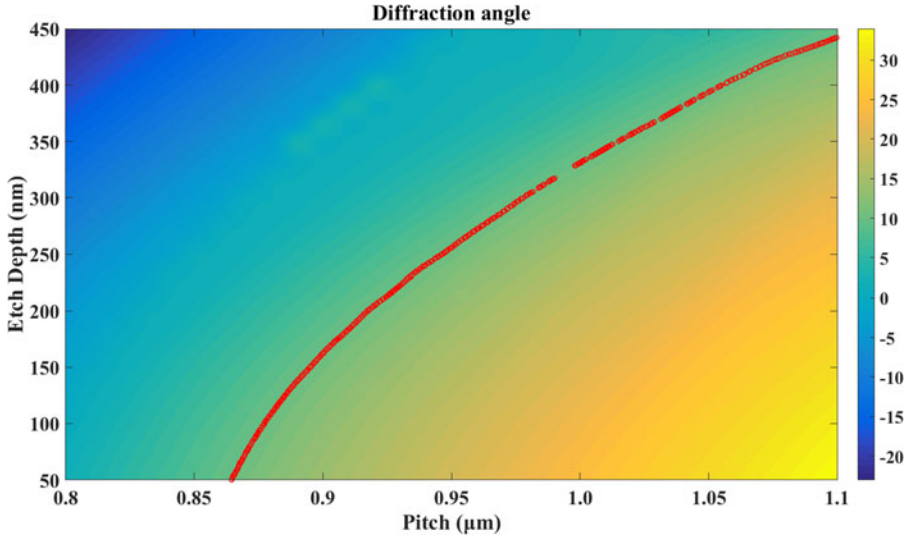

Fig. 2. Relationship between pitch, etch depth, and diffraction angle is depicted in this graph. While pitch and etch depth are given on x and y axis, respectively, the color in the background depicted the diffraction angle. The red dotted line, on the other hand, shows the values of pitch and etch depth for the diffraction angle of 10°.

This paper in Section 2 describes the simulation results, Section 3 delineates the process of fabrication of vertical coupler along with a ridge waveguide, Section 4 gives results and discussion of the achieved results, and Section 5 concludes the paper.

2. Simulating the Coupler

The design and optimization of the grating coupler was carried out in a Finite Difference Time Domain (FDTD). The design was set up using Silicon Dioxide as a substrate, with grating of Lithium Niobate on top of it. The 2-D set up of the simulation design is given in Fig. 1.

The top layer of Lithium Niobate has a height of 500 nm in our case, while that of Silicon Dioxide is 3 μm. The design can tolerate up to 10° tilt of the fibre from the vertical 90° without any significant loss in coupling efficiency. The relationship between etch-depth, pitch, and diffraction angle is give in Fig. 2.

Fig. 3, shows the coupling efficiency of the coupler with various etch depth values. The model maintains the pitch of the coupler to be constant and sweeps the etching depth of the coupler. The coupling efficiency maximizes to approximately 54% at the etching depth of 240 nm.

The optimized values for etching depth and Duty Cycle achieved after the optimization calculations are thus given in Table I.

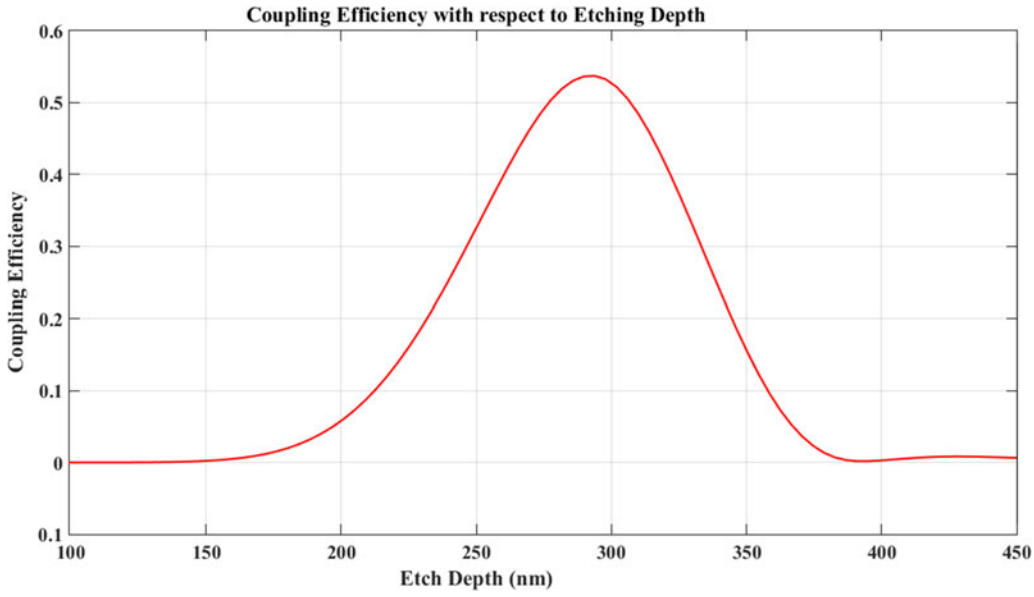

Fig. 3. With incident angle of 10° from the vertical axis, Coupling Efficiency versus etching depth at a fixed pitch of 950 nm.

TABLE 1
Values of etching depth and Duty Cycle used

Parameter	Optimized Value
d	279 nm
Duty Cycle	0.3

The coupling efficiency of the coupler, using the parameters given in Table I, was calculated for the entire C-band frequency spectrum and is given below in Fig. 4. The efficiency of the designed coupler reaches as high as −4.58 dB for the wavelength of 1530 nm. This efficiency then experiences a smooth rolls-off, reaching at its lowest of approximately −16 dB at the far end of the spectrum, at the wavelength of 1600 nm.

Fig. 4 further shows that within our desired range of 1530 nm to 1565 nm for C-band; the simulated coupling efficiency varies between −4.58 dB and −7.6 dB for the designed coupler. This is a fairly flat response for all the frequencies in the desired range.

3. Process of Fabrication

We used Lithium Niobate on Insulator (LNOI) substrate with a 450 nm thick layer of Lithium Niobate Thin Film (LNTF), buried layer of Silicon Dioxide with thickness of 1200 nm and a 0.5 mm thick Lithium Niobate handle wafer from NANOLN [27]. The fabrication process started with deposition of 20 nm thick titanium layer on top of the LNTF by the process of Electron Beam Evaporation (EBE). Layer of Titanium is added because of two reasons. First, Electron Beam resists have problem of adhesion on Lithium Niobate causing non-uniform layer of resist. This problem is eliminated by adding a layer of titanium on top of LNTF. Second, Lithium Niobate is a very bad conductor, which gives rise to the problem of connection error during Electron Beam Lithography (EBL) process.

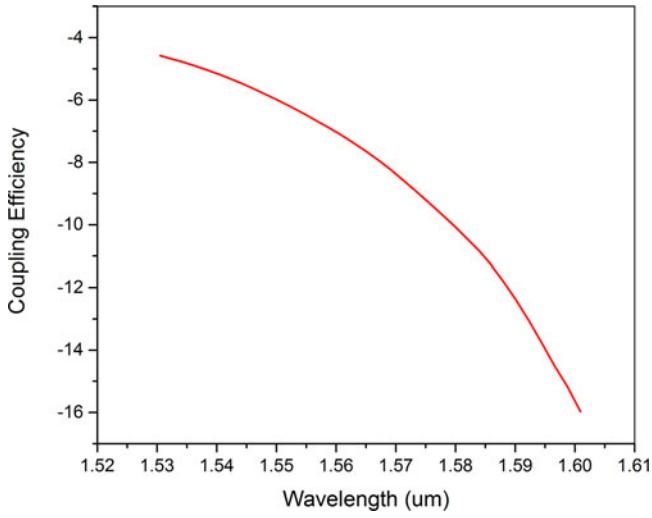

Fig. 4. Simulated Coupling Efficiency of the coupler.

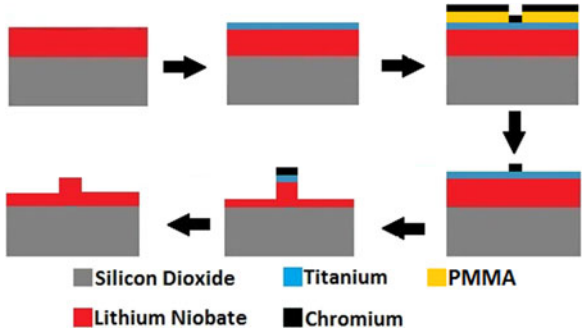

Fig. 5. Process flow for the fabrication of the ridge waveguide and the coupler.

Titanium is a known good conductor, addition of which removes the connection error in EBL process. PMMA, a positive tone resist, was then spin coated at 4000 rpm in order to achieve a 270 nm thick layer of resist. After spin coating, it was post- baked at 170 °C for 3 minutes. Electron Beam Lithography was performed on this wafer (with Vistec/EBPG5000plusES) in order to transfer the pattern on the wafer. The wafer retrieved from EBL process was then deposited with 80 nm thick Chromium using EBE in order to achieve a mask. After proper lift-off, the wafer was etched using Inductively Coupled Plasma (ICP) with Ar^+ ion and SF_6 as etchants, for approximately 7 minutes. This produced a ridge waveguide 700 nm wide along with a grating coupler. Next step was removal of Residual Chromium mask that still had a thickness of 46 nm. In order to remove the mask, it was at first placed in Sulphuric Acid at 117 °C for 15 minutes. The reaction of Sulphuric Acid with Chromium produces Chromium Sulphate, which is not soluble in water. Therefore, the sample was washed with Ethanol as Ethanol dissolves chromium sulphate leaving us with Lithium Niobate ridge waveguide and a coupler. The fabrication process flow is depicted in Fig. 5.

Energy Dispersive Analysis X-Ray(EDAX) test was carried out on the sample after completion of fabrication process to check any residual Chromium or Titanium on the top surface and the test turned out to be negative. The output of EDAX test, given in Fig. 6, shows different elements present in the sample with a spike. At the far right of this figure, there is a spike indicating presence of Boron. This actually is Lithium but as Lithium is a very light element and Boron is the lightest element that our machine can detect accurately, therefore, all of Lithium is either not detected or seen as Boron by the machine. The important thing here is that the test was carried out to check the presence of Titanium and Chromium. Both of these elements are sufficiently heavy to be detected

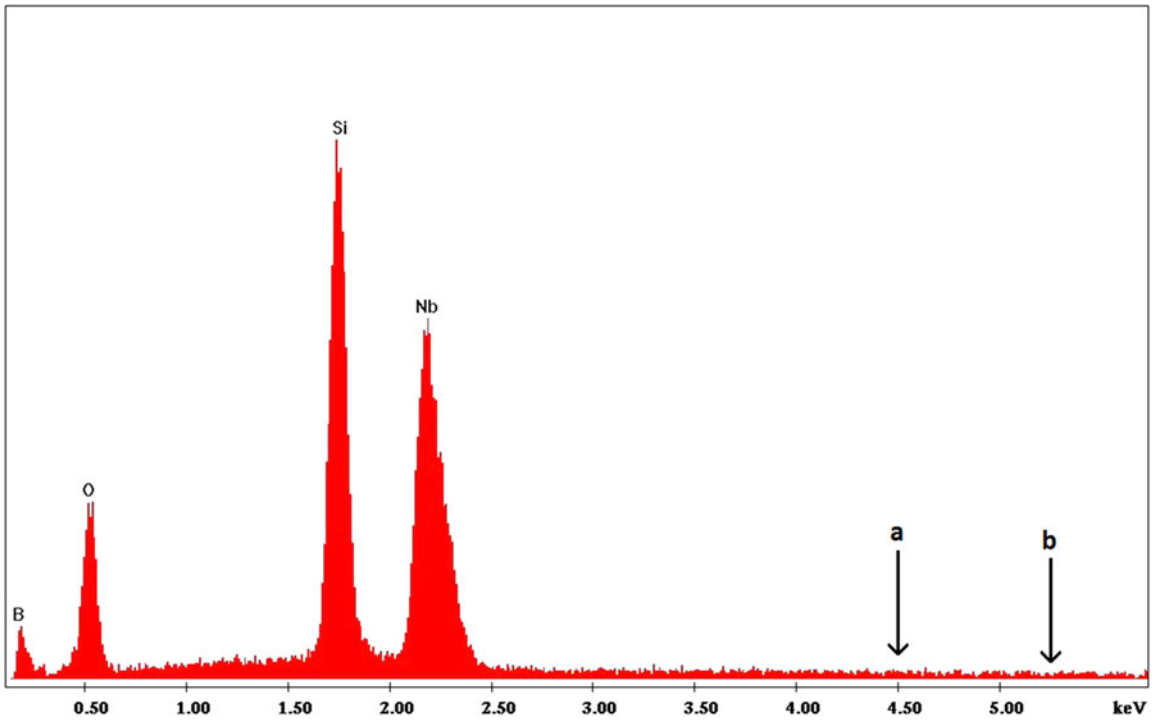

Fig. 6. EDAX test for the presence of Titanium and Chromium, which would have been depicted by peaks at points “a” and “b” [28] [29]

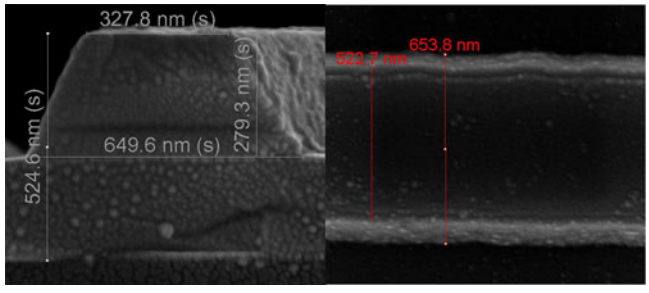

Fig. 7. Cross-section and top-view of the waveguide.

by our EDAX machine, and would have been indicated by peaks at points indicated as “a” and “b” in Fig. 6 [28], [29] . As no trace of both of these elements was found, it shows that we were successful in complete removal of all of residual Titanium and Chromium.

4. Results and Discussion

The fabrication process delineated above resulted in a waveguide with the height of 279.3 nm and width of 653.8 nm at the base. The Scanning Electron Microscope (SEM) images of cross-section and top-view of the waveguide are given in Fig. 7. The spots on the sample are due to deposition of gold on our sample. As Lithium Niobate is a non-conductive material, gold is sputter on it to achieve conductivity and thus capture SEM images.

The design of the coupler given in Fig. 8 is important, as it was difficult to fabricate the traditional design of the coupler. The side arms were added to the coupler in order to overcome the difficulty in the retention of coupler fins which otherwise was faced at the stage of lift-off of chromium. This addition provided us with a nearly perfect coupler with negligible effect on coupling efficiency.

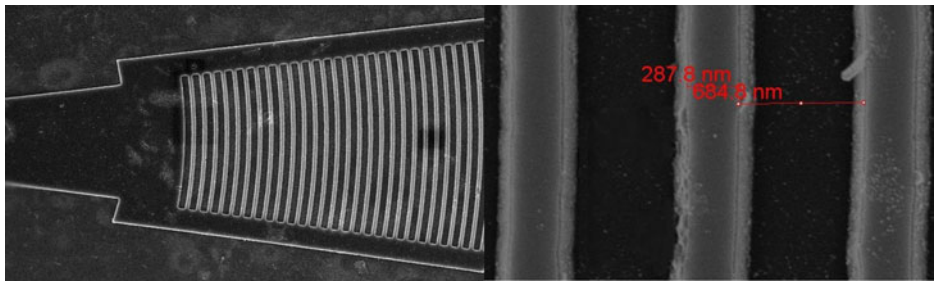

Fig. 8. Top view of the coupler and its close-up.

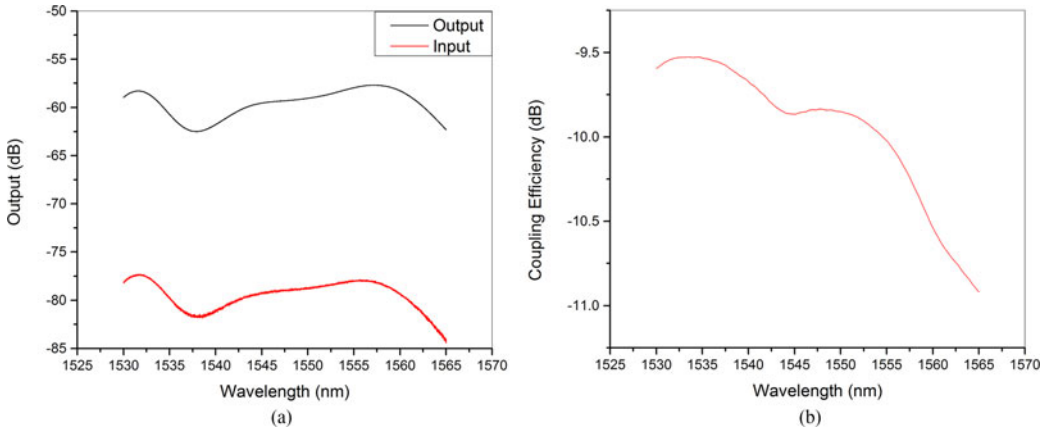

Fig. 9. (a) Spectrum of output and the source in dB. (b) Loss of a single coupler in dB.

The close-up of the coupler, given at the bottom of Fig. 8, shows the shortcomings of the etching process. The figure below shows that achieved coupler could not retain the desired duty-cycle of 50%. Moreover, the fabrication process leaves rough sidewalls and area in between two gratings.

The resulting coupler was tested on a test bench with a tunable laser source with a wavelength range of 1530 nm to 1630 nm and an optical spectrum analyser. The transverse electric (TE) polarization was selected from the laser source using a polarizer. The TE polarization was then fed to the coupler at an angle of 10° from the normal. The resulting output was obtained on the spectrum analyser from the coupler, as well as directly from the laser source for the purpose of subsequent analysis.

Fig. 9(a) shows the output obtained on the spectrum analyser directly from the source and through the coupler. As all couplers are inherently band pass filters, the fabricated coupler was no different. This pass band does corroborate with the C-band frequency spectrum of our desired design.

The graph in Fig. 9(a) translates into coupling efficiency of a single couplers using simple arithmetic and is depicted in Fig. 9(b). The coupling efficiency, given in Fig. 9(b), attains maximum value of approximately -9.45 dB at wavelength of 1537 nm. This efficiency of the coupler rolls-off to approximately as low as -11 dB at the far end of the spectrum (1565 nm).

The coupling efficiency of the fabricated coupler is less than the simulated coupling efficiency (given in Fig. 4) because of inconsistency of the fabricated coupler dimensions with the simulated coupler. These inconsistencies were introduced due to limitations of the fabrication process and the equipment. Three design parameters of a coupler are of crucial importance in order to achieve designed coupling efficiency. These three parameters are; duty cycle, etch depth and period or pitch of the grating. Figs. 7 and 8 clearly show that although these parameters of the fabricated coupler are close to their designed values but are not close enough to attain exactly the designed coupling efficiency.

Although it is always desirable to match the experimental results with the simulated results, but imperfections in the fabrication process due to technological bottlenecks always imply that the experimental results will usually be less than the prediction from theoretical models and simulation results. These technological shortcomings played their part in our fabrication process and did limit our coupling efficiency below the simulated coupling efficiency by approximately 5 dB.

5. Conclusion

This paper has presented theoretical and experimental results on grating couplers for coupling light between standard single-mode fibers and on chip waveguides. The couplers were also fabricated in LNOI. These couplers are suitable for the testing of photonic integrated components and circuits on the lithium niobate platform. In future more complex coupler designs can be explored in order to improve the coupling efficiency of the coupler.

References

[1] R. Geiss *et al.*, "Fabrication of nanoscale lithium niobate waveguides for second-harmonic generation," *Opt. Lett.*, vol. 40, pp. 2715–2718, 2015. doi: 10.1364/OL.40.002715.

[2] A. S. Solntsev *et al.*, "Cascaded third harmonic generation in lithium niobate nanowaveguides," *Appl. Phys. Lett.*, vol. 98, pp. 2011–2014, 2011. doi: 10.1063/1.3597627.

[3] G. D. Miller, "Periodically poled lithium niobate modeling, fabrication, and nonlinear optical performance," Ph.D. dissertation, Dept. Elect. Eng., Stanford Univ., Stanford, CA, USA, 1998. [Online]. Available: http://publication/uuid/DDE51384-5E09-4C05-AABE-3003DB9E0697.

[4] M. M. Fejer, D. H. Jundt, R. L. Byer, and G. A. Magel, "Quasi-phase-matched second harmonic generation: Tuning and tolerances," *IEEE J. Quantum Electron.*, vol. 28, no. 11, pp. 2631–2654, Nov. 1992. doi: 10.1109/3.161322.5

[5] R. L. Jungerman and C. A. Flory, "Low frequency acoustic anomalies in lithium niobate Mach–Zehnder interferometers," *Appl. Phys. Lett.*, vol. 53, 1988, Art. no. 1477.

[6] C. H. Bulmer, "Sensitive, highly linear lithium niobate interferometers for electromagnetic field sensing," *Appl. Phys. Lett.*, vol. 53, 1988, Art. no. 2368.

[7] J. Mathew, Y. Semenova, G. Rajan, and G. Farrell, "Humidity sensor based on photonic crystal fibre interferometer," *Electron. Lett.*, vol. 46 p, 1341, 2010, doi:10.1049/el.2010.2080.

[8] M. de Angelis *et al.*, "Evaluation of the internal field in lithium niobate ferroelectric domains by an interferometric method," *Appl. Phys. Lett.*, vol. 85, 2004, Art. no. 2785.

[9] P. Rabiei and W. H. Steier, "Lithium niobate ridge waveguides and modulators fabricated using smart guide," *Appl. Phys. Lett.*, vol. 86, pp. 1–3, 2005. doi: 10.1063/1.1906311.

[10] E. L. Wooten *et al.*, "A review of lithium niobate modulators for fiber-optic communications systems," *IEEE J. Sel. Top. Quantum Electron.*, vol. 6, no. 1, pp. 69–82, Jan./Feb. 2000. doi: 10.1109/2944.826874.

[11] D. A. Cohen, Lithium niobate microphotonic modulators, Ph.D. dissertation, Faculty Graduate School, Univ. Southern Calif., Los Angeles, CA, USA, 2001.

[12] I. P. Kaminow and E. H. Turner, "Electrooptic light modulators," *Proc. IEEE.*, vol. 54, no. 10, pp. 1374–1390, Oct. 1966. doi: 10.1109/PROC.1966.5124.

[13] W. Zhao *et al.*, "Efficient optical image amplifier using periodically poled lithium niobate," *Appl. Opt.*, vol. 54, pp. 9172–9176, 2015. doi:10.1364/AO.54.009172.

[14] A. C. Chiang *et al.*, "Pulsed optical parametric generation, amplification, and oscillation in monolithic periodically poled lithium niobate crystals," *IEEE J. Quantum Electron.*, vol. 40, no. 6, pp. 791–799, Jun. 2004. doi:10.1109/JQE.2004.828269.

[15] J. Kiessling, R. Sowade, I. Breunig, K. Buse, and V. Dierolf, "Cascaded optical parametric oscillations generating tunable terahertz waves in periodically poled lithium niobate crystals," *Opt. Exp.*, vol. 17, pp. 87–91, 2009. doi: 10.1364/OE.17.000087.

[16] G. S. Kanter, P. Kumar, K. R. Parameswaran, and M. M. Fejer, "Wavelength-selective pulsed all-optical switching based on cascaded second-order nonlinearity in a periodically poled lithium-niobate waveguide," *IEEE Photon. Technol. Lett.*, vol. 13, no. 4, pp. 341–343, Apr. 2001. doi: 10.1109/68.917845.

[17] J. M. Dawlaty, F. Rana, and W. J. Schaff, "Ultrafast all-optical switches based on intersubband transitions for Tb/s operation," in *Proc. SPIE 5597*, Nanophotonics for Communication: Materials and Devices, Oct. 25, 2004, pp. 56–61, doi:10.1117/12.571436.

[18] R. Weis and T. Gaylord, "Lithium niobate: Summary of physical properties and crystal structure," *Appl. Phys. A Mater. Sci. Process.*, vol. 37, pp. 191–203, 1985. doi: 10.1007/BF00614817.

[19] O. Yavuzcetin *et al.*, "Photonic crystal fabrication in lithium niobate via pattern transfer through wet and dry etched chromium mask," *J. Appl. Phys.*, vol. 112, 2012, Art. no. 074303. doi: 10.1063/1.4756958.

[20] H. Hu, R. Ricken, W. Sohler, and R. B. Wehrspohn, "Lithium niobate ridge waveguides fabricated by wet etching," *IEEE Photon. Technol. Lett.*, vol. 19, no. 6, pp. 417–419, Mar. 2007. doi: 10.1109/LPT.2007.892886.

[21] Y. Li, C. Wang, and M. Loncar, "Design of nano-groove photonic crystal cavities in lithium niobate," *Opt. Lett.*, vol. 40, pp. 2902–2905, 2015, doi: 10.1364/OL.40.002902.

[22] L. Wang *et al.*, "Selective etching in LiNbO3 combined of MeV O and Si ion implantation with wet-etch technique," *Surf. Coatings Technol.*, vol. 201, pp. 5081–5084, 2007. doi: 10.1016/j.surfcoat.2006.07.145.
[23] D. Taillaert *et al.*, "An out-of-plane grating coupler for efficient butt-coupling between compact planar waveguides and single-mode fibers," *IEEE J. Quantum Electron.*, vol. 38, no. 7, pp. 949–955, Jul. 2002. doi: 10.1109/JQE.2002.1017613.
[24] C. J. Brooks, A. P. Knights, and P. E. Jessop, "Vertically-integrated multimode interferometer coupler for 3D photonic circuits in SOI," *Opt. Exp.*, vol. 19, pp. 2916–2921, 2011. doi: 10.1117/12.763470.
[25] G. Y. Jung, J. Yongsik, C. Sunkyu, and Y. Kyounghoon, "A new compact 3-D hybrid coupler using multi-layer mierostrip lines at 15 GHz," in *Proc. 36th Eur. Microw. Conf., 2006*, pp. 25–28. doi: 10.1109/EUMC.2006.281172.
[26] K. Kawase, M. Sato, T. Taniuchi, and H. Ito, "Coherent tunable THz-wave generation from LiNbO3 with monolithic grating coupler," *Appl. Phys. Lett.*, vol. 68, pp. 2483–2485, 1996. doi: 10.1063/1.115828.
[27] M. Levy *et al.*, "Fabrication of single-crystal lithium niobate films by crystal ion slicing," *Appl. Phys. Lett.*, vol. 73, pp. 2293–2295, 1998. doi: 10.1063/1.121801.
[28] B. R. Sankapal, M. Ch. Lux-Steiner, and A. Ennaoui, "Synthesis and characterization of anatase-TiO2 thin films," *Appl. Surface Sci.*, vol. 239, pp. 165–170, 2005. doi: 10.1016/j.apsusc.2004.05.142.
[29] V. Murphy, S. A. M. Tofail, H. Hughes, and P. McLoughlin, "A novel study of hexavalent chromium detoxification by selected seaweed species using SEM-EDX and XPS analysis," *Chem. Eng. J.*, vol. 148, pp. 425–433, 2009. doi: 10.1016/j.cej.2008.09.029.